ACS APPLIED MATERIALS & INTERFACES

Research Article

www.acsami.org

Room Temperature Self-Healing Thermoset Based on the Diels–Alder Reaction

Purnomo A. Pratama,[†] Majid Sharifi,[†] Amy M. Peterson,[†,‡] and Giuseppe R. Palmese*,[†]

[†]Department of Chemical & Biological Engineering, Drexel University, 3141 Chestnut Street, Philadelphia, Pennsylvania 19104, United States

[‡]Department of Chemical Engineering, Worcester Polytechnic Institute, 100 Institute Road, Worcester, Massachusetts 01609, United States

ABSTRACT: A self-healing epoxy-amine thermoset based on the compatible functionalization of the thermoset and encapsulated healing agent has been successfully developed. Healing of the thermoset resulted from the reaction of furans in the thermoset and multimaleimides (MMIs) in the healing agent solution. The healing agent, MMI dissolved in phenyl acetate, was encapsulated using a urea-formaldehyde encapsulation method. Autonomic healing of the thermoset was achieved by incorporating microcapsules filled with the healing agent solution within a furan-functionalized epoxy-amine thermoset. The resulting self-healing thermoset recovered 71% of its initial load after fracture.

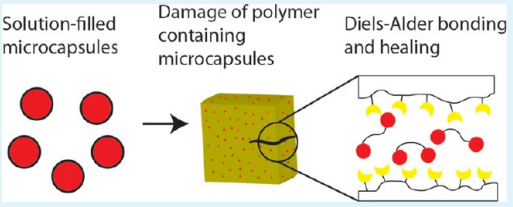

KEYWORDS: *self-healing polymers, Diels–Alder, microencapsulation, epoxy-amine thermosets, composites*

INTRODUCTION

Wound healing is an incredibly useful ability of biological systems. It requires living things to sense and repair damage over a range of length and time scales.[1−5] While very complex, healing allows living things to live longer and be more active. Inspired by the natural healing process, much research has been devoted to developing materials capable of self-healing.[6−9] Healing of thermosetting polymers is of particular interest. While thermosets are widely used in load-bearing applications because of their high strength and environmental stability, they are brittle and susceptible to cracking. Self-healing of thermosets is particularly desirable for applications where damage detection is difficult, where replacing damaged materials is not cost-effective, and where material failure is a safety concern.[10,11] Interest in self-healing materials has been high over the past decade, as shown by the numerous reviews written on this topic.[12−17]

The two primary healing methodologies in polymers have focused on either incorporation of a healing agent or dynamic bonds within the network. White et al. developed the healing agent method for thermosetting polymers.[6] Using a urea-formaldehyde (UF) encapsulation method, microcapsules filled with dicyclopentadiene (DCPD) were formed. These microcapsules and Grubbs' catalyst were incorporated within a thermosetting network. Upon fracture of the polymer, microcapsules ruptured, releasing DCPD into the crack surface. When exposed to Grubbs' catalyst, DCPD underwent ring-opening metathesis polymerization (ROMP) and healed the crack. Recovery of approximately 85% of the virgin fracture toughness was reported in the first study. Permutations of the healing agent method include using solvents,[18] solutions,[19−23] poly(dimethyl siloxane)[24] or tung oil[25] as healing agents. Additionally, tubular,[26−29] vascular,[30−35] and electrospun[36] systems for healing agent storage have also been investigated.

The pioneering work in polymer healing based on dynamic bonds was performed by Chen et al.[9] Thermosets were synthesized in which cross-links were formed through reversible Diels–Alder bonding between furan and maleimide. The initial materials showed an average load recovery of 80% after fractured specimens were subjected to heat treatment. Another method of healing based on the Diels–Alder reaction was proposed by Peterson et al., who prepared a healable epoxy-amine thermoset.[22] A furan-bearing monomer was added to the resin mixture, providing furan functional groups to the resulting thermoset. Healing was achieved with direct injection of a bismaleimide solution in the crack surface, which resulted in covalent Diels–Alder bonding across the crack as well as swelling-induced physical interlocking of the crack faces. Seventy percent of initial load was recovered after healing at room temperature for 12 h. Pratama et al. investigated this system further by examining the role of healing agent properties on healing efficiency of the system as well as the system's application as a healable coating.[19,37]

In the work of Peterson et al. and Pratama et al., the healing agent was manually injected at the damage site.[19,22,37] While significant load recovery was obtained, these studies focused on exploring the parameters significantly for healing of furan-functionalized thermosets with multimaleimides in solution and only demonstrated a proof-of-concept. The current work builds on the previous studies and reports on the preparation and characterization of autonomously healing furan-functionalized

Received: August 17, 2013
Accepted: November 11, 2013
Published: November 11, 2013

thermosets containing encapsulated multimaleimide (MMI) solutions as the healing agent. This study focuses on the selection of a suitable healing agent solvent, dispersion of the resulting capsules, and evaluation of the healing efficiency of capsule-containing thermosets. This is the first report of an autonomically healing thermosetting system based on the Diels–Alder reaction.

EXPERIMENTAL SECTION

Materials. Epoxies diglycidyl ether of bisphenol A (DGEBA, EPON 828, Miller Stephenson) and furfuryl glycidyl ether (FGE, Sigma Aldrich) were combined and cured with a stoichiometric amount of the amine curing agent biscyclohexanamine (PACM, Air Products). Fumed silica (Cab-o-sil) was used to improve microcapsule dispersion by modifying resin viscosity. Healing agents were prepared by dissolving MMIs in phenyl acetate (PA, Sigma Aldrich). In the current work, three different MMIs were used: 1,1′-methylenedi-4,1-phenylene)bismaleimide (MMI-1, Sigma-Aldrich); 1,6′-bismaleimido-2,2,4-trimethylhexane (MMI-2, Daiwakasei Industries, Japan via Miki Sangyo U.S.A.); poly(phenylmethanemaleimide) (n = 0.5), (MMI-3, Daiwakasei Industries Japan via Miki Sangyo U.S.A.). Chemical structures of many of the compounds used are provided in Table 1.

Table 1. List of Several Chemical Structures Used in This Work

Name	Structure
DGEBA n = 0.13	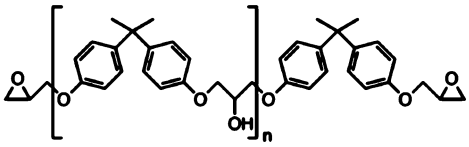
FGE	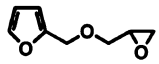
PACM	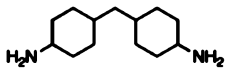
MMI-1	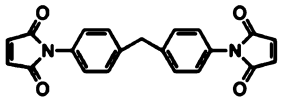
MMI-2	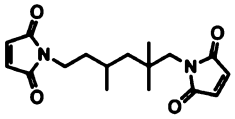
MMI-3 n = 0.5	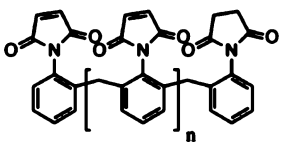

Healing agents were encapsulated in UF microcapsules using an oil-in-water emulsion process. The chemicals used for microcapsule synthesis include urea, ammonium chloride, resorcinol, 36% formaldehyde solution, and 2 M aqueous sodium hydroxide, all from Sigma-Aldrich and used without additional purification. Additionally, the surfactant ethyl maleic anhydride polymer (EMA, Zemac E-400) was obtained from Vertellus.

Encapsulation Procedure. The encapsulation of healing agent using UF capsules is based on previous work from Brown et al. and Blaiszik et al.[38,39] Slight modifications were made to their procedures to improve yield. First, 200 mL of deionized water was mixed with 25 mL of 2.5 wt % EMA solution in a 600 mL beaker. Then, 2.5 g of urea, 0.25 g of resorcinol, and 0.25 g of ammonium chloride were dissolved sequentially into the reaction mixture. The solution pH was subsequently adjusted from 2.7 to 3.5 using 2 M sodium hydroxide. After that, the solution was placed in an oil bath at room temperature and was mechanically stirred while the healing agent solution (a MMI in PA) was slowly added. The resulting emulsion was stirred at 500 rpm for at least 5 min, after which time 6.33 g of 36% formaldehyde solution was added. The temperature of the oil bath was raised to 55 °C and maintained at 55 °C for 4 h to allow for the formation of UF capsule walls around healing agent droplets. The solution was subsequently removed from the oil bath and allowed to cool while stirred at room temperature for an additional 6 h to ensure complete capsule formation. The resulting mixture was filtered using coarse filter paper designed to recover particles 1 μm or larger. The recovered product was washed twice with deionized water and twice with acetone. The water wash steps removed water-soluble components of the emulsion, while the acetone washes removed nonencapsulated PA and MMI and decreased microcapsule aggregation. The filtered and washed capsules were air-dried for 48 h before sieving and use.

Polymer Preparation. Furan-functionalized thermosets were prepared by curing a 3:2 by weight ratio of DGEBA and FGE with a stoichiometric amount of PACM. Resins were mixed using a THINKY planetary mixer at 2000 rpm for 4 min, with a subsequent degassing step of 800 rpm for 1 min. Once mixed, resins were poured into the appropriate molds and cured for 2 h at 60 °C and postcured for 2 h at 90 °C.[22] This system will be denoted as DGEBA-FGE-PACM. Microcapsules were incorporated by adding capsules to the already mixed resin and mixing the resulting system for 1 min at 2000 rpm, followed by 30 s of degassing at 800 rpm. Scanning electron microscopy (SEM) micrographs of polymer fracture surfaces were obtained at least one week after testing to ensure that any solvent-induced swelling has subsided so that the fracture surfaces would be representative of the virgin and fully healed conditions.

Capsule Characterization. An optical microscope coupled with ImageJ (National Institute of Health) analysis was used to determine average microcapsule size. Representative samples (>150 data points per condition) were used to determine capsule diameters under varying conditions. PA content within microcapsules was determined with thermogravimetric analysis (TGA). Specimens were heated at a rate of 10 °C min^{-1} to 200 °C, at which point specimens were held at 200 °C for 1 h. The temperature of 200 °C was selected for the isothermal condition based on the PA's boiling point at 196 °C. PA content was taken as the mass loss during TGA testing.

Gel Permeation Chromatography (GPC) was used to determine the composition of the capsule content.[20] Capsules were placed within the barrel of a syringe with a filter of pore size 0.45 μm attached. Capsules were crushed by the plunger, and the liquid ejected through the filter tip was diluted by 100× with tetrahydrofuran (THF). The diluted solution was injected in a GPC column with a THF flow rate of 1.00 mL min^{-1}. Healing agent concentration inside capsules was determined using a calibration curve based on the elution profiles of standard solutions containing known concentrations of MMI in PA.

Swelling Study. Polymer swelling studies were performed on DGEBA-FGE-PACM under different conditions. As described in previous work, spherical polymer specimens were prepared and immersed in 1 mL of solvent.[19] Solvent mass uptake was recorded daily, and the results were used to determine swelling (S), as shown in eq 1.

$$S = \frac{M_t}{M_0} \times 100\% \quad (1)$$

S is swelling, M_t is the sample mass at time t, and M_0 is the initial mass of the specimen.

Compact Tension Test. Healing efficiency was evaluated using modified contact tension specimens in accordance with ASTM D 5045-99. This testing procedure has been described previously by Chen et al., Peterson et al., and others.[22,40−42] A crack-arresting hole was introduced to prevent crack propagation through the whole length

of the specimen. This improves realignment of crack surfaces. A precrack was introduced by running a fresh razor blade across the base of the notch. Uniaxial tensile loading was applied to the specimens until fracture using an Instron 8872 at a loading rate of 0.4 mm min^{-1}.[22]

For healing via direct application of the healing agent, 10 μL of healing agent was injected into the fracture surface. Specimens were healed at room temperature under minimal pressure (≈5.5 kPa) for 24 h.[41,22] Following healing, specimens were loaded to failure for the second time. Healing efficiency for each specimen was calculated using eq 2.

$$\eta_h = \frac{P_h}{P_0} \times 100\% \quad (2)$$

In this expression, η is healing efficiency, P_h is the maximum load for the healed specimen (second loading), and P_0 is the maximum load for initial fracture of the same specimen. All healing efficiency results are presented as averages of at least five tested specimens with error bars representing standard deviations.

RESULTS AND DISCUSSION

Solvent Selection. Previous work indicates that selection of an appropriate solvent is necessary to maximize the healing efficiency of furan-functionalized epoxy-amine thermosets.[19,37] The solvent must be capable of both swelling the polymer matrix and dissolving MMI species. In previous studies, dimethylformamide (DMF) and toluene were investigated. Although both solvents demonstrate the aforementioned criteria, they are unsuitable for encapsulation using the UF method because of the miscibility of DMF in water and the volatility of toluene. A solvent appropriate for encapsulation must satisfy two additional criteria: Immiscibility in water and low volatility.[37]

PA showed great potential as a healing agent solvent because it satisfies all four criteria. It has a relatively high boiling point and is immiscible in water. In addition, it is able to dissolve MMI molecules and swell the polymer network, as shown in Tables 2 and 3, respectively. Maximum concentrations in Table 2 represent saturation concentration at 22 °C.

Table 2. Maximum Concentration of MMIs in Various Solvents

	maximum concentration (M)		
MMI structure	DMF	toluene	PA
MMI-1	0.58	N/A	0.13
MMI-2	1.16	0.295	0.40
MMI-3	1.46	N/A	0.42

Table 3. Maximum Solvent Uptake of the DGEBA-FGE-PACM Network in Various Solvents

solvent	swelling
DMF	170% ± 5%
toluene	39% ± 3%
PA	151% ± 24%

Healing via Direct Application of Healing Agent. Previous studies have shown that healing of DGEBA-FGE-PACM systems using a healing agent solution containing MMIs is dependent on MMI concentration, solvent choice, and healing time.[37,22] Figure 1 shows healing efficiency as a function of MMI-2 concentration for the DGEBA-FGE-PACM system containing 1% Cab-o-sil. Healing agent was directly injected in the crack site for these experiments. Healing efficiency increased with MMI-2 concentration, following the same trend as healing with MMI-2 in DMF as previously reported by Pratama et al.[37] Eighty percent healing efficiency was obtained for samples healed with the maximum concentration of MMI-2 in PA (0.4 M), while 43.7% healing efficiency was observed for samples healing with pure PA. This high healing efficiency for pure PA is obtained in a fully cured thermosetting network because the glass transition temperature (T_g) of the network is relatively low (54 °C).[22] In previous work, the same healing efficiencies were achieved for the DGEBA-FGE-PACM system and a furan-free analogue with an identical cross-link density when both were healing via direct injection of DMF.[22]

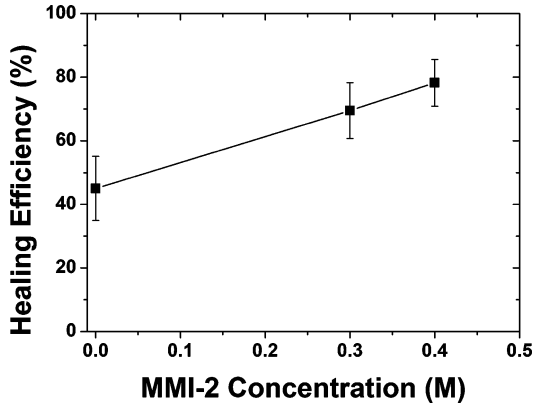

Figure 1. Healing efficiency as a function of MMI-2 concentration in PA. Specimens were healed for 24 h.

In Figure 2, the healing efficiency of three healing agent solutions (PA-based, DMF-based, and toluene-based healing agents) is compared. MMI-2 concentration was kept constant at 0.295 M, and healing time was kept at 24 h. PA and PA-based healing agents yielded higher healing efficiencies than the other solvents. Seventy percent load recovery was achieved when specimens were healed with 0.295 M MMI-2 dissolved in PA.

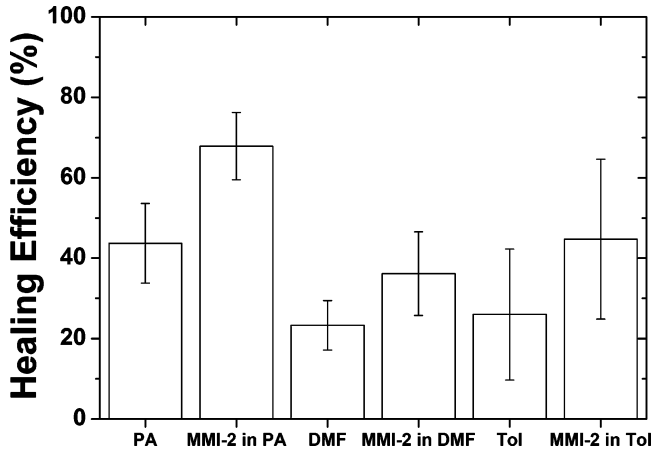

Figure 2. Comparison of healing efficiency for direct injection of PA-based, DMF-based, and toluene-based healing agent solutions and the corresponding solvents into a crack surface. Healing agent solutions consisted of 0.295 M MMI-2 dissolved in the appropriate solvent. Specimens were healed for 24 h.

The effect of healing time on load recovery was also investigated. The healing efficiency of PA and 0.295 M MMI-2

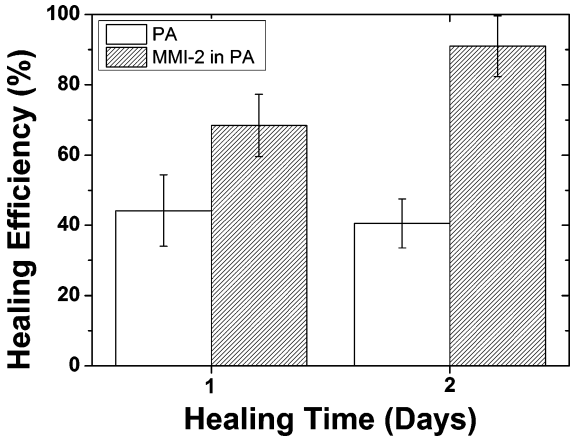

Figure 3. Comparison of healing efficiency for direct injection of healing agent after 1 and 2 days of healing time. Healing agent solution was 0.295 M MMI-2 in PA.

after 1 and 2 days is compared in Figure 3. An increase in healing efficiency at longer healing times was observed for specimens healed with MMI-2 in PA, while the healing efficiency of pure PA did not change with time. Longer healing time allowed for further reaction between maleimides and furans across the fracture surface, resulting in increased healing efficiency.[37] Recovery of over 90% of the initial strength was observed for specimens healed with 0.295 M MMI-2 after 2 days of healing.

Capsule Properties. Blaiszik et al. showed that PA could be encapsulated in UF capsules. They obtained spherical microcapsules with diameters of approximately 100 μm at an agitation rate of 500 rpm.[20] While microcapsules filled with MMI-3 dissolved in PA have successfully been synthesized, this work focuses only on encapsulation of MMI-2 dissolved in PA and the healing efficiency of the resulting self-healing materials. This choice was made because MMI-2 demonstrated the highest healing efficiency in a previous study of MMIs in DMF.[37] Microcapsules filled with healing agent solution were prepared with 0.13 M MMI-2. Figure 4 shows the optical microscopy images of UF microcapsules filled with 0.13 M MMI-2 synthesized at an agitation rate of 500 rpm.

Encapsulation of higher concentration MMI-2 solutions could not be achieved. Precipitation of the BMI from the emulsion and low yields of microcapsules were observed when the synthesis of microcapsules filled with higher concentration MMI-2 solutions was attempted. We believe that these problems arise from preferential solubility of the emulsion components in PA as compared to MMI-2.

Figure 5 consists of histograms showing the distribution of diameters for capsules filled with pure PA and with 0.13 M MMI-2. The average diameter for microcapsules filled with PA is 185 $\pm$ 33 μm, while the average diameter for microcapsules filled with 0.13 M MMI-2 is 181 $\pm$ 49 μm. Capsule diameters, size distribution, and morphology are consistent with previous work on UF microcapsules synthesized at similar agitation rates.[20]

TGA of microcapsules filled with PA showed that the PA content was 88% by weight. Capsule morphology was investigated using SEM. Microcapsules exhibit a smooth inner wall and rough outer wall, as shown in Figure 6. This morphology has been previously observed and results from the capsule synthesis procedure.[43,20] A continuous, smooth

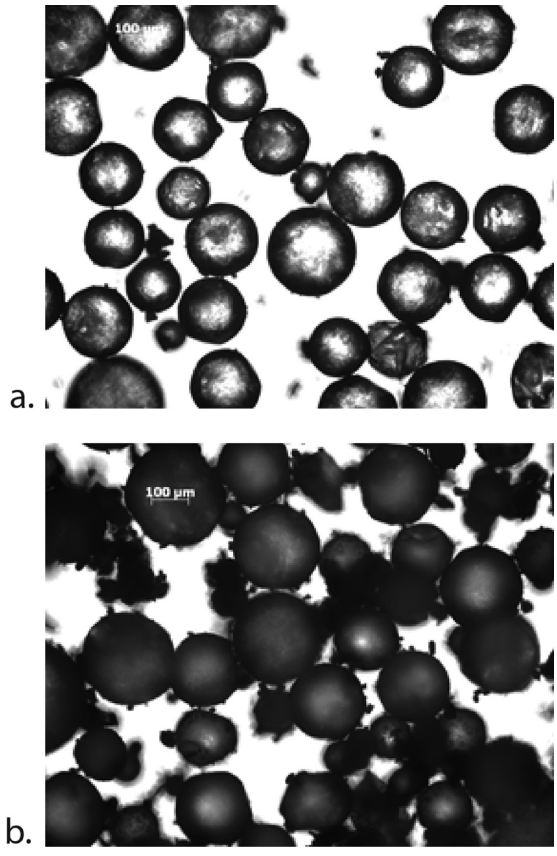

Figure 4. Optical micrographs of microcapsules filled with (a) PA and (b) 0.13 M MMI-2.

membrane is formed at the water−oil interface as urea and formaldehyde react in the water phase and form a low molecular weight polymer. As the reaction progresses, colloidal urea-formaldehyde particles form in the aqueous phase and are deposited along the interface. This creates the rough outer wall.

GPC was used to analyze capsule content. Healing agent concentration was calculated by measuring the relative peak area at the elution times corresponding to the MMI and the solvent species. Results are shown in Table 4. MMI-2 concentration was found to increase after encapsulation, suggesting some amount of PA evaporation during capsule synthesis. The known concentration of the MMI-2 solution prior to encapsulation was confirmed with the GPC-based calibration curves, further validating this method.

Dispersion of Capsules. The main challenge in incorporating microcapsules within a polymer matrix is ensuring good dispersion. Mixing monomers and capsules initially resulted in a homogeneous mixture. However, capsules floated to the top during the curing process, leading to high- and low-concentration phases instead of a well-dispersed system. Heterogeneous dispersion became more apparent with increasing capsule loading.

To prevent uneven distribution of capsules, the rheological properties of the resin were modified through the addition of Cab-o-sil. Cab-o-sil is a fumed silica additive and has been widely used to adjust viscosity with minimal change in other properties.[44−47] The addition of 1−2 wt % Cab-o-sil significantly improved the dispersion of capsules throughout the thermoset. An SEM micrograph of fracture surfaces of DGEBA-FGE-PACM with 1 wt % Cab-o-sil and 10 wt %

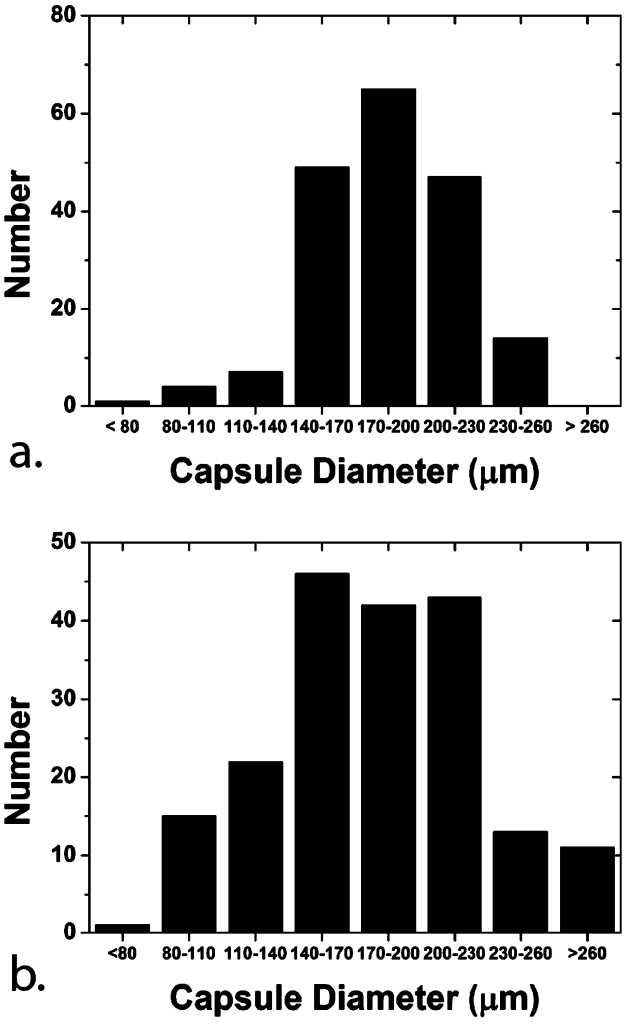

Figure 5. (a) Distribution of diameters for capsules filled with PA (Sample size: 187 capsules); (b) distribution of diameter for capsules filled with MMI-2 in PA (sample size: 193 capsules).

capsule content is shown in Figure 7. SEM verifies good dispersion of capsules throughout the epoxy thermoset in the presence of Cab-o-sil. Good dispersion could also be observed visually. Cab-o-sil increased the viscosity of the resin and allows the capsules to remain suspended throughout the entire sample volume prior to network gelation. In addition, it was observed that adding 1 wt % Cab-o-sil did not significantly affect the swelling behavior of DGEBA-FGE-PACM when immersed in PA. Maximum solvent uptake increases slightly, from 151% to 186%.

Self-Healing via Microcapsule Incorporation. Self-healing thermosetting polymers were prepared by incorporating encapsulated healing agent in the furan-functionalized thermoset. Specimens for testing of self-healing ability consisted of 1 wt % Cab-o-sil and 10 wt % microcapsules in a DGEBA-FGE-PACM resin matrix. A healing efficiency of 71% was obtained for specimens containing capsules with MMI-2 in PA, while only 43% healing efficiency was observed with capsules containing just PA. Results are summarized in Figure 8. The results demonstrated the successful development of a truly self-healing system based on the Diels–Alder reaction using encapsulated maleimide solutions as healing agent incorporated within a furan-functionalized epoxy-amine.

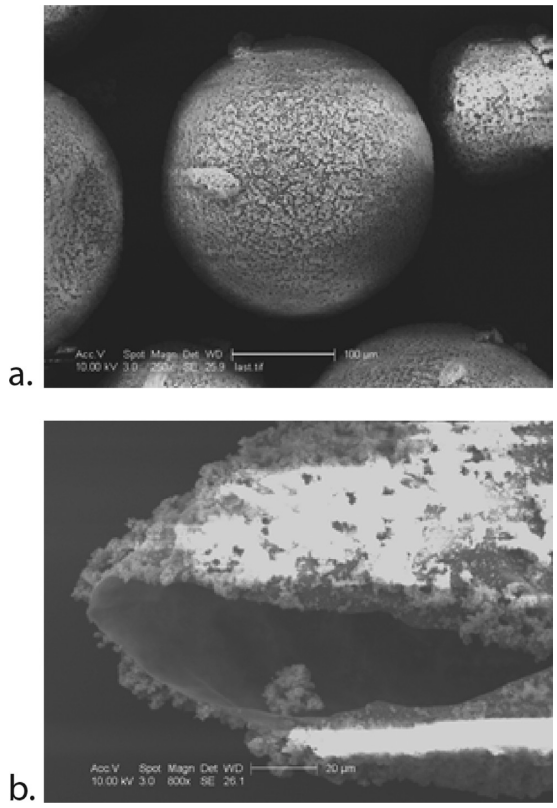

Figure 6. SEM images of (a) intact and (b) sliced microcapsules filled with PA.

Table 4. Concentration of Healing Agent Inside the Capsule from GPC Test

	relative area (%)		
sample description	PA	MMI-2	MMI-2 (M)
before encapsulation	96.94	3.06	0.13
after encapsulation	96.18	3.82	0.16

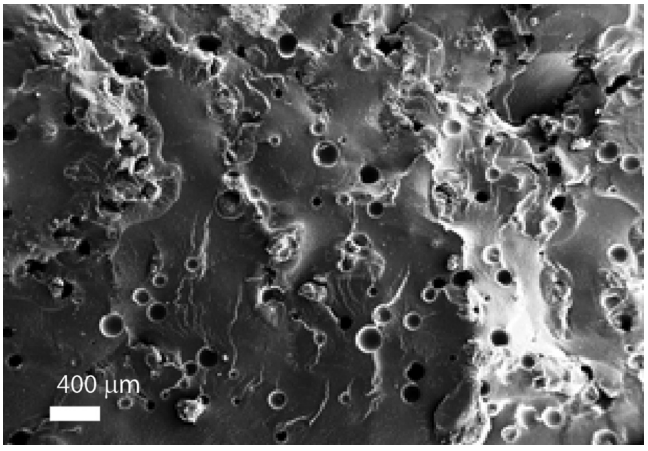

Figure 7. Fracture surface of DGEBA-FGE-PACM with 10 wt % capsule and 1 wt % Cab-o-sil.

Since different MMI-2 concentrations were used for the injection and capsule procedures (0.295 M vs 0.13M), the results cannot be directly compared. Figure 8 shows healing efficiency as a function of MMI-2 concentration for both techniques. Healing efficiencies of injected and encapsulated

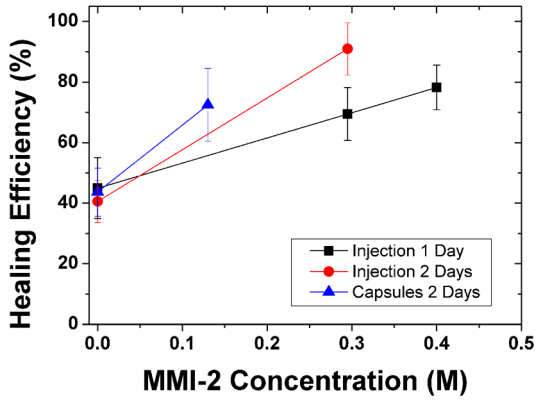

Figure 8. Comparison of healing efficiency between self-healing systems healed with injection of healing agents (PA and MMI-2 in PA) and capsules filled with these healing agent solutions.

pure solvent are the same. Interestingly, the autonomic (capsule-based) healing technique demonstrates comparable healing efficiencies (within error) to the direct injection technique at lower MMI-2 concentrations. Healing via direct injection may require higher concentrations of MMI-2 to achieve similar healing efficiency results to autonomic healing because of the greater solvent volume used for direct injection healing and the resulting lower strength of the swelled epoxy-amine network.

CONCLUSIONS

The development of a solution-based self-healing system based on compatible functionalization of the healing agent and polymer network using Diels–Alder reactive groups has been reported. Peterson et al. initially demonstrated the healing potential of such systems.[22] Pratama et al. expanded on this idea by analyzing the solvent and solution diffusion profiles and reaction kinetics as well as the applicability of such a system in healable coatings.[19] In a subsequent study, Pratama et al. investigated the effects of healing agent properties such as solvent selection, healing time, healing agent concentration and structure on healing efficiency.[37] Finally, the current work investigated the encapsulation of a maleimide solution healing agent and evaluated the healing efficiency of this self-healing system. The healing agent solution MMI-2 in PA has been successfully encapsulated in UF shells. These spherical microcapsules were dispersed in a furan-functionalized epoxy-amine thermoset to provide healing agent solution to provide self-healing to the thermoset. Capsule dispersion was improved by the addition of fumed silica as a viscosity modifier. The resulting thermoset containing MMI-2 solution-filled capsules recovered on average 71% of the initial load. Ongoing work includes overcoming the problems associated with encapsulating higher concentration MMI-2 solutions and investigating the healing ability of microcapsules containing solutions of other MMIs. Future directions for this work include healing optimization and expanding the applicability of this healing paradigm to other thermosets.

AUTHOR INFORMATION

Corresponding Author

*E-mail: palmese@coe.drexel.edu. Phone: (215) 895-2227.

Notes

The authors declare no competing financial interest.

ACKNOWLEDGMENTS

The authors wish to acknowledge the U.S. Army Research Laboratory for financial support under the Army Materials Center of Excellence Program, contract W911NF-06-2-0013. The authors also thank James Throckmorton for assistance with collecting SEM images.

REFERENCES

(1) Singer, A. J.; Clark, R. A. F. *New Engl. J. Med.* **1999**, *341*, 738–746.
(2) Martin, P. *Science* **1997**, *276*, 75–81.
(3) Faria, P. E. P.; Carvalho, A. L.; Felipucci, D. N. B.; Wen, C.; Sennerby, L.; Salata, L. A. *Clin. Implant Dent. R.* **2010**, *12*, 72–79.
(4) Lee, J. Y.; Qu-Petersen, Z.; Cao, B.; Kimura, S.; Jankowski, R.; Cummins, J.; Usas, A.; Gates, C.; Robbins, P.; Wernig, A.; Huard, J. *J. Cell Biol.* **2000**, *150*, 1085–1100.
(5) Eriksson, C.; Broberg, M.; Nygren, H.; Oster, L. *J. Biomed. Mater. Res. A* **2003**, *66*, 662–668.
(6) White, S. R.; Sottos, N. R.; Geubelle, P. H.; Moore, J. S.; Kessler, M. R.; Sriram, S. R.; Brown, E. N.; Viswanathan, S. *Nature* **2001**, *409*, 794–797.
(7) Granger, S.; Loukili, A.; Pijaudier-Cabot, G.; Chanvillard, G. *Cem. Concr. Res.* **2007**, *37*, 519–527.
(8) Leibler, L.; Cordier, P.; Soulie, C. *Nature* **2008**, *451*, 977–980.
(9) Chen, X.; Dam, M. A.; Ono, K.; Mal, A.; Shen, H.; Nutt, S. R.; Sheran, K.; Wudl, F. *Science* **2002**, *295*, 1698–1702.
(10) Pang, J.; Bond, I. P. *Composites, Part A* **2005**, *36*, 183–188.
(11) Williams, G. J.; Bond, I. P.; Trask, R. S. *Composites, Part A* **2009**, *40*, 1399–1406.
(12) Wool, R. P. *Soft Matter* **2008**, *4*, 400–418.
(13) Blaiszik, B. J.; Kramer, S. L. B.; Olugebefola, S. C.; Moore, J. S.; Sottos, N. R.; White, S. R. *Annu. Rev. Mater. Sci.* **2010**, *40*, 19.1–19.33.
(14) Bergman, S. D.; Wudl, F. *J. Mater. Chem.* **2008**, *18*, 41–62.
(15) Wu, D. Y.; Meure, S.; Solomon, D. *Prog. Polym. Sci.* **2008**, *33*, 479–522.
(16) Herbst, F.; Döhler, D.; Michael, P.; Binder, W. H. *Macromol. Rapid Commun.* **2013**, *34*, 203–220.
(17) Hager, M. D.; Greil, P.; Leyens, C.; van der Zwaag, S.; Schubert, U. S. *Adv. Mater.* **2010**, *22*, 5424–30.
(18) Caruso, M. M.; Delafuente, D. A.; Ho, V.; Sottos, N. R.; Moore, J. S.; White, S. R. *Macromolecules* **2007**, *40*, 8830–8832.
(19) Pratama, P. A.; Peterson, A. M.; Palmese, G. R. *Macromol. Chem. Phys.* **2012**, *213*, 173–181.
(20) Blaiszik, B. J.; Caruso, M. M.; McIlroy, D. A.; Moore, J. S.; White, S. R.; Sottos, N. R. *Polymer* **2009**, *50*, 990–997.
(21) Caruso, M. M.; Blaiszik, B. J.; White, S. R.; Sottos, N. R.; Moore, J. S. *Adv. Funct. Mater.* **2008**, *18*, 1898–1904.
(22) Peterson, A. M.; Jensen, R. E.; Palmese, G. R. *ACS Appl. Mater. Interfaces* **2010**, *2*, 1141–1149.
(23) McIlroy, D. A.; Blaiszik, B. J.; Caruso, M. M.; White, S. R.; Moore, J. S.; Sottos, N. R. *Macromolecules* **2010**, *43*, 1855–1859.
(24) Keller, M. W.; White, S. R.; Sottos, N. R. *Adv. Funct. Mater.* **2007**, *17*, 2399–2404.
(25) Kumar, A.; Stephenson, L.; Murray, J. *Prog. Org. Coat.* **2006**, *55*, 244–253.
(26) Trask, R. S.; Williams, G. J.; Bond, I. P. *J. R. Soc. Interface* **2007**, *4*, 363–371.
(27) Kousourakis, A.; Mouritz, A. P. *Smart Mater. Struct.* **2010**, *19*, 85021.
(28) Pang, J.; Bond, I. P. *Compos. Sci. Technol.* **2005**, *65*, 1791–1799.
(29) Dry, C. *Smart Mater. Struct.* **1994**, *3*, 118–123.
(30) Williams, H. R.; Trask, R. S.; Knights, A. C.; Williams, E. R.; Bond, I. P. *J. R. Soc. Interface* **2008**, *5*, 735–747.
(31) Hamilton, A. R.; Sottos, N. R.; White, S. R. *J. R. Soc. Interface* **2012**, *9*, 1020–1028.
(32) Hansen, C. J.; Wu, W.; Toohey, K. S.; Sottos, N. R.; White, S. R.; Lewis, J. A. *Adv. Mater.* **2009**, *21*, 4143–4147.

(33) Hansen, C. J.; White, S. R.; Sottos, N. R.; Lewis, J. A. *Adv. Funct. Mater.* **2011**, *21*, 4320−4326.
(34) Toohey, K. S.; Sottos, N. R.; Lewis, J.; Moore, J. S.; White, S. R. *Nat. Mater.* **2007**, *6*, 581−585.
(35) Dong, H.; Esser-Kahn, A. P.; Thakre, P. R.; Patrick, J. F.; Sottos, N. R.; White, S. R. *ACS Appl. Mater. Interfaces* **2012**, *4*, 503−509.
(36) Park, J.-H.; Braun, P. V. *Adv. Mater.* **2009**, *22*, 496−499.
(37) Pratama, P. A.; Peterson, A. M.; Palmese, G. R. *Polym. Chem.* **2013**, *4*, 5000−5006.
(38) Brown, E. N.; Kessler, M. R.; Sottos, N. R.; White, S. R. *J. Microencapsulation* **2003**, *20*, 719−730.
(39) Blaiszik, B. J.; Sottos, N. R.; White, S. R. *Compos. Sci. Technol.* **2007**, *68*, 978−986.
(40) Chen, X.; Wudl, F.; Mal, A.; Shen, H.; Nutt, S. *Macromolecules* **2003**, *36*, 1802−1807.
(41) Peterson, A. M.; Jensen, R. E.; Palmese, G. R. *ACS Appl. Mater. Interfaces* **2009**, *1*, 992−995.
(42) Rahmathullah, M. A. M.; Palmese, G. R. *J. Appl. Polym. Sci.* **2009**, *113*, 2191−2201.
(43) Keller, M. W.; Sottos, N. R. *Exp. Mech.* **2006**, *46*, 725−733.
(44) Ferch, H. K. In *Colloidal Silica: Fundamentals and Application*; Bergna, H. E., Roberts, W. O., Eds.; CRC Press: Boca Raton, FL, 2006; Chapter 14, pp 187−192.
(45) Gun'ko, V. M.; Zarko, V. I.; Sheeran, D. J.; Blitz, J. P.; Leboda, R.; Janusz, W.; Chibowski, S. *J. Colloid Interface Sci.* **2002**, *252*, 109−118.
(46) Snyder, F.; Stephens, N. *Anal. Biochem.* **1962**, *4*, 128−131.
(47) Braun, D. D.; Rosen, M. R. *Rheology Modifiers Handbook: Practical Use and Application*; William Andrews Publishing: Norwich, NY, 2008; pp 168−170.